UDK: 007.52:741.5:004.6/7
COSATI: 13-06,17-07

Influence of the Construction Type of a Cable-Suspended Parallel Robot on its Kinematic and Dynamic Model

Mirjana Filipović[1)]
Ana Djurić[2)]
Ljubinko Kevac[3)]

The presented Cable-suspended Parallel Robot named the RFCPR system is an important and attractive outcome for the engineering and scientific community due to its future intensive development. The proper definition of the system kinematic model which includes trajectory, velocity and acceleration is a prerequisite for the formulation of a dynamic model. These three components represent the basic functional criteria of the real system which is described by the corresponding geometric relations and differential equations. The relationship between external and internal forces is defined by the Lagrange principle of virtual work. The Jacobian matrix is directly involved in the application of the Lagrange principle of virtual work and the generation of the dynamic model of the RFCPR system. The system construction defines its kinematic and dynamic models. The ORVER software package is used for a comparative analysis of dynamic responses of the observed configurations. Two different examples of the RFCPR system are analyzed and their results are presented. The application possibilities are certainly much broader than it may be assumed at this moment, especially for military or police purposes

Key words: **robotized system, cable-suspended robot, cable connection, model analysis, kinematic analysis, dynamic analysis, Lagrange principle, Jacobian matrix, software.**

Designations

DOF	– degree of freedom
CPR	– Cable-suspended Parallel Robot
RFCPR	– Rigid ropes F-type Cable-suspended Parallel Robot
$t(s)$	– time
$dt(s)$	– sample time
$g=(\mathrm{m/s^2})$	– gravitational acceleration
$p=[x \;\; y \;\; z]^T$	– position of the camera carrier in the Cartesian space
$i=1,2,3$	– total number of DOF
$\varphi=[\theta_1 \;\; \theta_2 \;\; \theta_3]^T$	– vector of the internal coordinates
$\theta_i(\mathrm{rad})$	– motor shaft angular position after the gear box
$F_F=[F_1 \;\; F_2 \;\; F_3]^T$	– forces in the ropes (main forces)
$F_p=[F_x \;\; F_y \;\; F_z]^T$	– acting forces on the camera carrier
$P_p=[P_{px} \;\; P_{py} \;\; P_{pz}]^T$	– perturbation forces acting on the camera carrier
$M_F=[M_1 \;\; M_2 \;\; M_3]^T$	– motors load moments (main load moments)
$R_i(\mathrm{m})$	– winch radius
J_F	– Jacobian matrix
$R_{ri}(\Omega)$	– rotor circuit resistance
$u_i(V)$	– voltage
$i_i(A)$	– rotor current
$C_{Ei}(V/(\mathrm{rad/s}))$	– back electromotive force constant
$C_{Mi}(\mathrm{Nm/A})$	– constant of the moment proportionality
$B_{Ci}(\mathrm{Nm/(rad/s)})$	– coefficient of viscous friction
$J_{ri}(\mathrm{kgm^2})$	– moment of inertia for the rotor and the gear box
$G_{vi}=\frac{J_{ri}\cdot R_{ri}}{C_{Mi}}$	– motor inertia characteristic
$L_{vi}=\frac{R_{ri}\cdot B_{Ci}}{C_{Mi}}+C_{Ei}$	– motor damping characteristic
$S_{vi}=\frac{R_{ri}}{C_{Mi}}$	– motor geometric characteristic
$m(\mathrm{kg})$	– mass of the camera carrier
$d(\mathrm{m})$	– length of the recorded field
$s(\mathrm{m})$	– width of the recorded field
$v(\mathrm{m})$	– height of the recorded field
$\delta\theta_{i\Xi}$ (rad), $\delta\dot{\theta}_{i\Xi}$ (rad/s)	– initial deviation of the motor angular position
K_{lpi}, K_{lvi}	– positional, velocity amplification for motion control
$\Diamond$	– factor that characterizes two parallel guided ropes

Introduction

A system for the observation of the workspace with moving objects has been developed to some extent and widely analyzed in various research areas as well as for

[1)] University of Belgrade, Institute of Mihailo Pupin, Volgina 15, 11060 Belgrade, SERBIA
[2)] Wayne State University, 4855 Fourth St. Detroit, MI 48202, USA
[3)] University of Belgrade, Innovation center School of Electrical Engineering, Bulevar Kralja Aleksandra 73, 11000 Belgrade, SERBIA

different applications. Similar systems were analyzed and modeled as presented by numerous publications.

The kinematic design of a planar three-degree-of-freedom parallel manipulator is considered in paper [16]. Four optimal different design criteria are established and analyzed. A trajectory planning approach for cable-suspended parallel mechanisms has been presented in [17]. A planar two-degree-of-freedom parallel mechanism has been used in the analysis. Paper [3] studied the kinematics and statics of under-constrained cable-driven parallel robots with less than six cables, in a crane configuration. In these robots, kinematics and statics are intrinsically coupled and they must be dealt with simultaneously. A motion controller for a six DOF tendon-based parallel manipulator (driven by seven cables), which moves a platform with high speed, is introduced in [7]. The workspace conditions and the dynamics of the manipulator are described in details. In paper [1], the authors presented the algorithms that enable a precise trajectory control of the Networked Info Mechanical Systems - NIMS, and an under constrained three-dimensional -3D cabled robot intended for use in actuated sensing. They provide a brief system overview and then describe methods to determine the range of operations of the robot. Several prototypes of the wire-driven parallel robots, with different actuation schemes, have been presented in [30]. Two of them have been evaluated through extensive tests and they showed unexpected kinematic problems. The wrench-closure workspace of parallel cable-driven mechanisms is the set poses of their mobile platform for which the cables can balance any external wrench. The determination of this workspace is an important issue in [18] since the cables can only pull and not push on the mobile platform. Parallel cable-driven Stewart-Gough platforms consist of an end-effector which is connected to the machine frame by motor driven cables. Since cables can transmit only tension forces, at least $m = n + 1$, cables are needed to tense a system having n degrees-of-freedom. This will cause a kinematical redundancy and lead to a $(m - n)$ - dimensional solution space for the cable force distribution presented in [2]. The recent result from a newly designed parallel wire robot which is currently under construction is presented in [33]. It has been used for developing a new technique for computation and transfer of its workspace to the available CAD software. An auto-calibration method for over constrained cable-driven parallel robots using internal position sensors located in the motors has been presented in [31]. A calibration workflow is proposed and implemented including pose selection, measurement, and parameter adjustment. The wire-driven parallel robot presented in [27] has attracted the interest of researchers since the very beginning of the study of parallel robots. This type of robot has the advantage of having light mobile mass, simple linear actuators with a possibly relatively large stroke and less risk of interference between the legs. On the other hand, their major drawback is that the wire actuator can only pull and not push. Paper [32] addressed the issue of control design for a redundant 6-DOF cable robot with positive input constraints. The design is based on a feedback linearization controller named reference governor - RG. A nonlinear dynamic analysis of the suspended cable system is carried out with some sensible results presented in [6] that could be useful to real LSRT (Large Spherical Radio Telescopes) engineering. Integrated mechanical, electronic, optic and automatic control technologies are employed to make considerable improvement upon the same system. A multiple cable robotic crane designed in [37] is used to provide improved cargo handling. The equations of motion are derived for the cargo and flexible cable using Lagrange's equations and the assumed modes method. The results are compared against the desired cable lengths and the results achieved in the previous research using a rigid cable model. This is one of a few papers dealing with flexible ropes. For the requirement of the trajectory tracking of the LSRT, a large fine tuning platform based on the Stewart platform is presented in papers [38] and [39]. The mathematical model for the kinematic control is developed with coordinate transformation, and a dynamic analysis is made using a Jacobian matrix, which, with a singularity analysis, built a solid base for the tracking control. Paper [29] addresses the static analysis of the cable-driven robotic manipulators with the non-negligible cable mass. An approach to computing the static displacement of a homogeneous elastic cable is presented. The resulting cable-displacement expression is used to solve the inverse kinematics of general cable-driven robotic manipulators. The cable suspended parallel robot is analyzed in [41], in which cables are utilized to replace links to manipulate objects. It is developed from parallel and serial cable-driven robots. Compared with parallel robots, this type of robots has more advantages. The cooperative variation of lengths of six cables pulls the feed cabin to track a radio source with six degrees of freedom. The cable-driven parallel manipulator can only bear tension, but not compression. Therefore, a cable system with j end-effectors DOFs requires at least $(j+1)$ cables as shown in [28]. For three-translational motions of the feed in the system, a four-cable-driven parallel manipulator has been developed. For the design of the five-hundred-meter aperture spherical radio telescope, a four-cable-driven parallel manipulator, which is long in span and heavy in weight, is adopted as the first-level adjustable feed-support system. The goal of paper [40] is to optimize the dimensions of the four-cable-driven parallel manipulator to meet the workspace requirement of the constraint condition in terms of cable tension and stiffness.

However, the same CPR can be used for many other purposes, and one of them is the observation of workspace.

The motion of the camera carrier was controlled by the operator using a joystick.

Functionality of this system significantly depends on operator's concentration and responsibility. Their skill and experience played a major role. Since the implementation of task observation of an event can last for hours, it was a big responsibility for operators. A lack of concentration and their fatigue during this period indicated a significant dependence of this system on the human factor, which as a result could have a number of unavoidable inaccuracies during the operation.

In the current literature survey, there is no mathematical model of the Cable-suspended Parallel Robots with double parallel ropes and there is no available procedure for generating the Jacobian matrix of similar systems. Another problem is that the current published models do not include the motors dynamics. The analysis and synthesis of these complex systems cannot be proper without the motor dynamics, because it represents the dominant dynamics for any electro mechanical system.

The kinematic formulation of the presented RFCPR system is a key contribution in this paper, which will be used for the system realization. This formulation can be used for determining the Jacobian matrix of any CPR system configuration. This methodology for developing the kinematic model of selected CPR systems is named the

KinCPR-Solver (Kinematic Cable-suspended Parallel Robot Solver), and it gives precise direct and inverse kinematic solutions.

The dynamic model is generated using the fundamental dynamic theory based on the Lagrange's principle of virtual work. The mathematical model of the motors is determined using the Lagrange's equations and expressed with the generalized coordinates.

In this paper, the camera carrier workspace has the shape of a parallelepiped, such that the camera carrier hangs over the ropes properly connected on the four highest points i.e. the four upper angles of the workspace. The suspension system is defined in these four points.

A camera workspace is an area where the camera can move quietly and continuously by following the observed object.

A camera carrier moves freely in the 3D space which enables the recording of the object from the above.

This gives a unique feeling to the viewer to follow the event easily from an unusual proximity and to be very close to the action regardless of the size of the observed space.

This paper analyzes the mechanism which involves only the positioning of the camera carrier. It is assumed that the camera orientation can be determined using the already known, smaller mechanism with three DOF. In this case, a camera carrier has a mechanism for defining the camera orientation and the camera is installed on the top of this mechanism. For large workspace, this should be an optimal solution.

The camera motion is controlled by the ropes which are synchronized by three motors.

Ropes are unwinding (or winding) and that makes the camera able to reach any position in the 3D space.

The control system provides a three-dimensional motion of the camera. The commands for the synchronized motion of each winch are provided, with the control of the motion of each motor, which ultimately provides three-dimensional continuous camera carrier motion. A gyro sensor, installed in the camera carrier, is stabilized towards the horizon.

As many robotic systems, the CPR is very complex and includes many subsystems. The simplest dynamic model of such system involves a series of subsystems which interact with each other, and also it involves the interaction forces, compatibility conditions of displacement and kinetic parameters of the system dynamics.

In this sense, the rheonomic coordinates method is used for the dynamic modeling and the control of the camera moving along a specific path in the CPR model along a programmed and controlled trajectory.

Since there are elements such as axially movable cables which have transversal oscillations in this model, it is necessary to study first specific elements of the CPR system, such as the transverse vibrations of axially moving ropes. Classical models of transversal oscillations of axially moving belts and ropes are given, for example, in papers [34-36]. The analytical presentations of the descriptions of their own and forced transverse oscillations of axially moving sandwich belts, as well as the energetic analysis, are given in references [19-26]. This can be further used in a studious analysis of the camera model dynamics in order to define the rope movable manipulator position and orientation.

Future researches include implementation of the features of elastic ropes (type of nonlinear dynamic elasticity as defined in [8-14]) in the mathematical model of the CPR.

In this research, several different CPR models will be unified according to their similarities into one reconfigurable model, using the approaches presented in [4] and [5].

In this paper, the real system abstraction will be used for modeling purposes by neglecting the transverse vibrations of the ropes (un-stretchable ropes).

The first paper that relates to one type of the CPR system that was previously published in a Serbian journal is paper [15]. This paper shows the existence of the singularity conditions for the CPR-A system. This problem appears in the area close to the workspace boundaries, where the oscillations appear without any perturbations in the system response.

Concerning the wide possibility of the CPR applications, as well as future development of the system, there is an urgent need for this research. Therefore, the goal of this research is to implement the CPR model which will move in the 3D space with a high accuracy.

In Section 2, a detailed description of the RFCPR system is given and devoted to the RFCPR kinematic model, which is directly involved in the development of its dynamic model. Two cases of the system responses are analyzed for different conditions in Section 3. In Section 4, the concluding remarks are presented.

Mathematical model of the RFCPR system

In this research, one subsystem of the CPR family has been selected and analyzed in depth. The graphical representation of that system, named RFCPR, is shown in Fig.1.

The Camera carrier of the RFCPR structure is guided through the work area of the parallelepiped shape with three ropes connected with three winches, each powered by motor.

The ropes of the pulley system are run on the winches (reels) 1, 2, 3, powered by motors. The ropes coil or uncoil on the winches of radius R_1, R_2, and R_3. The motors rotate winches directly and their angular positions are θ_1, θ_2, θ_3. This motion moves the camera in the x, y, z Cartesian coordinates. This represents the desired motion trajectory of the camera carrier.

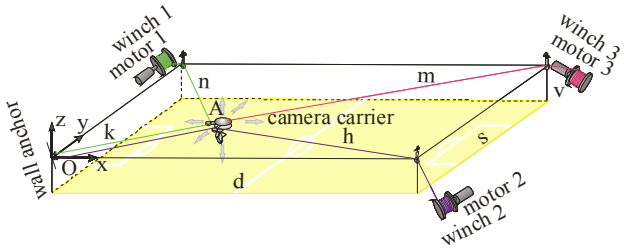

Figure 1. RFCPR, in the 3D space

The first step towards the dynamic model of the RFCPR is the development of its kinematic model. This calculation involves an accurate definition of the geometric relationship between the camera motion in the Cartesian x, y, z space (external coordinates) and the motor angular positions θ_1, θ_2, θ_3, (internal coordinates).

The relation between the internal and external coordinates is defined by the Jacobian matrix J_F, which relates the velocities of the external coordinates $\dot{p} = [\dot{x} \;\; \dot{y} \;\; \dot{z}]^T$ with the velocities of the internal coordinates $\dot{\varphi} = [\dot{\theta}_1 \;\; \dot{\theta}_2 \;\; \dot{\theta}_3]^T$. For the generation of any trajectory in the x, y, z space, it is necessary to provide a very precise and mutually coordinated motion of all three motors θ_1, θ_2, θ_3.

The 3D recorded space has a parallelepiped shape of the length d, width s, and height v. In this 3D space it can be seen that the camera is connected with the ropes. See Fig.2. The connecting dimensions are δ_{x1}, δ_{x2}, δ_{y1}, δ_{y2}. These dimensions are very small in comparison with the complete 3D recorded space. From this observation it is clear that $\delta_{x1} \approx 0$, $\delta_{x2} \approx 0$, $\delta_{y1} \approx 0$, $\delta_{y2} \approx 0$. It is also assumed that the pivot point A height z is equal to the heights of all three connecting points.

This fact allows us to choose a point A as a hanging position of the camera carrier for all three ropes, see Fig.2. This camera carrier system can be easily constructed. This assumption simplifies the definition of the geometric relations between the camera carrier motion in the Cartesian coordinates and the coordinated motions of all the motors.

The relationship which connects the velocities of the external coordinates $\dot{p} = [\dot{x} \;\; \dot{y} \;\; \dot{z}]^T$ with the velocities of the internal coordinates $\dot{\varphi} = \left[\dot{\theta}_1 \;\; \dot{\theta}_2 \;\; \dot{\theta}_3\right]^T$, is presented in equation (1).

$$\dot{\varphi} = J_F \cdot \dot{p} \tag{1}$$

$$J_F = \begin{bmatrix} J_{F11} & J_{F12} & J_{F13} \\ J_{F21} & J_{F22} & J_{F23} \\ J_{F31} & J_{F32} & J_{F33} \end{bmatrix} \tag{2}$$

This procedure is named KinCPR-Solver (Kinematic Cable-suspended Parallel Robot Solver). The Jacobian matrix J_F in equation (1) is a full matrix. The elements of this matrix beyond the diagonal show the strong coupling between the external and internal coordinates.

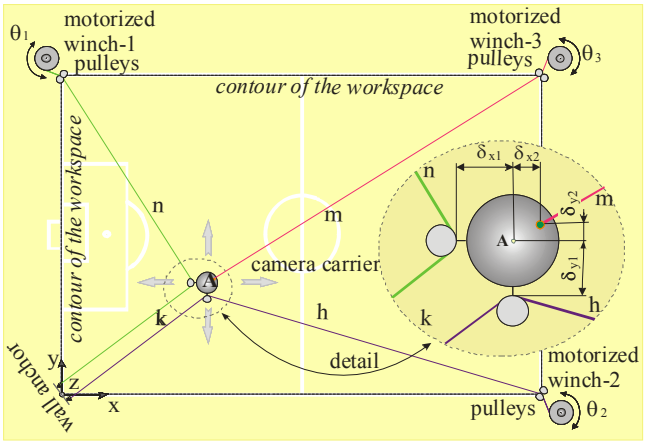

Figure 2. RFCPR, top view

The camera carrier together with the camera represents a small system in comparison to the complete work area. In that case, the small system has negligible moments of inertia about each axis of the local coordinate system at the point A.

For the camera dynamics modeling, the camera is presented as a material particle with 3 DOF in the x, y, z Cartesian coordinates system.

The kinetic energy E_k and the potential energy E_p of the camera carrier motion with the mass m are given in the following equations:

$$E_k = \frac{1}{2} \cdot m \cdot \dot{x}^2 + \frac{1}{2} \cdot m \cdot \dot{y}^2 + \frac{1}{2} \cdot m \cdot \dot{z}^2 . \tag{3}$$

$$E_p = m \cdot g \cdot z . \tag{4}$$

In this analysis, the ropes are assumed to be rigid. In that case, the mathematical model of the described system has the following form:

$$u = G_v \cdot \ddot{\varphi} + L_v \cdot \dot{\varphi} + S_v \cdot M_F \tag{5}$$

The vector equation (5) is developed by applying the Lagrange's equation on the generalized coordinates θ_1, θ_2, θ_3.

Where: $u = [u_1 \;\; u_2 \;\; u_3]^T$, $G_{v(3x3)} = diag\, G_{vi}$, $L_{v(3x3)} = diag\, L_{vi}$, $S_{v(3x3)} = diag\, S_{vi}$.

The main load moment M_F is defined with the vector's equation (6).

$$M_F = \begin{bmatrix} F_1 \cdot R_1 \\ F_2 \cdot R_2 \\ F_3 \cdot R_3 \end{bmatrix}. \tag{6}$$

The main force includes the three components expressed in a vector form below.

$$F_F = \begin{bmatrix} F_1 \\ F_2 \\ F_3 \end{bmatrix} \tag{7}$$

The next step is to describe the dynamic balance between the main force F_F (or the main moment M_F) and the external force F. See Figures 2 and 3.

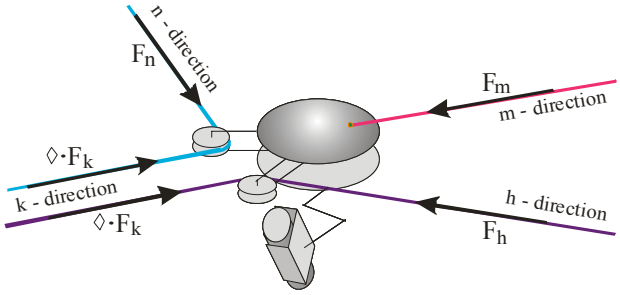

Figure 3. The ropes forces carry a camera

Two similar right-angle triangles in the $x-k$ plane are presented in the 2D space. See Fig.4a. These triangles in the $x-k$ plane can be seen in the 3D space shown in Fig.4b.

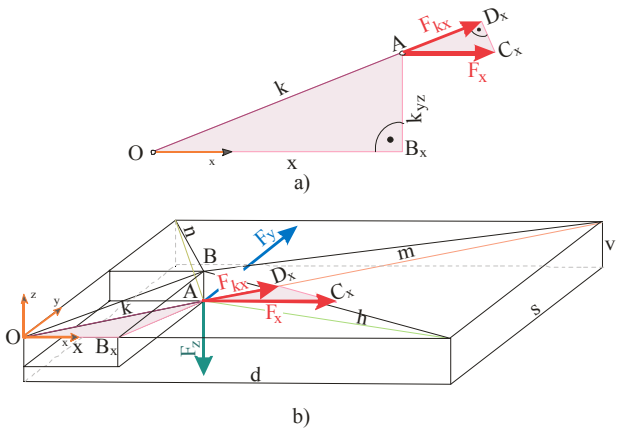

Figure 4. a) A characteristic triangle in the $x-k$ plane, b) A characteristic triangle in the 3D space

The hypotenuse of the OAB_x triangle has the length k, which is changeable during the camera motion.

The other two sides of the OAB_x triangle have the sizes x and $K_{yz} = \sqrt{y^2 + z^2}$.

The component of the external force F in the x direction is F_x and the projection of the force F_x on the k direction is F_{kx} which can be seen in Fig.4.

The similarities of the two triangles in Fig.4 produce the following relations:

$$\frac{x}{k} = \frac{F_{kx}}{F_x}. \tag{8}$$

$$F_{kx} = \frac{x}{k} \cdot F_x. \tag{9}$$

In Fig.5, another two similar right-angled triangles are shown.

These triangles are placed in the y - k plane.

The two sides of the OAB_y triangle have the sizes y and $K_{xz} = \sqrt{x^2 + z^2}$. The component of the external force F in the y direction is F_y and the projection of the force F_y on the k direction is F_{ky} which can be seen in Fig.5.

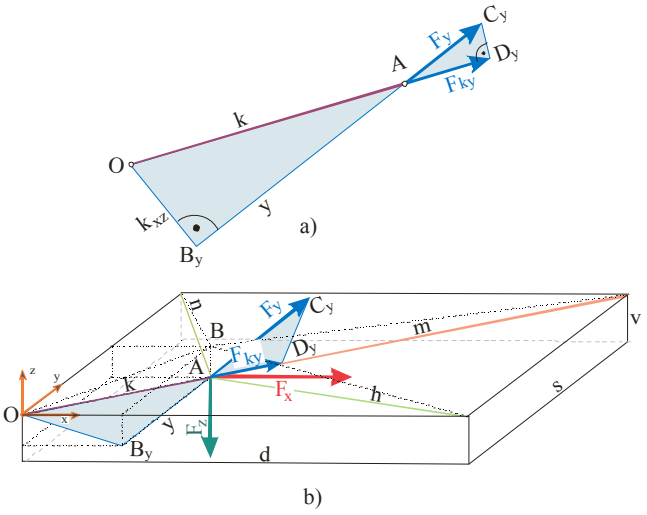

Figure 5. a) A characteristic triangle in the y - k plane, b) A characteristic triangle in the 3D space

The similarities of the two triangles in Fig.5 produce the following relations:

$$\frac{y}{k} = \frac{F_{ky}}{F_y}. \tag{10}$$

$$F_{ky} = \frac{y}{k} \cdot F_y. \tag{11}$$

In Fig.6, two more similar right-angled triangles are shown. These triangles are in the z - k plane.

The hypotenuse of the OAB_z triangle has the length k.

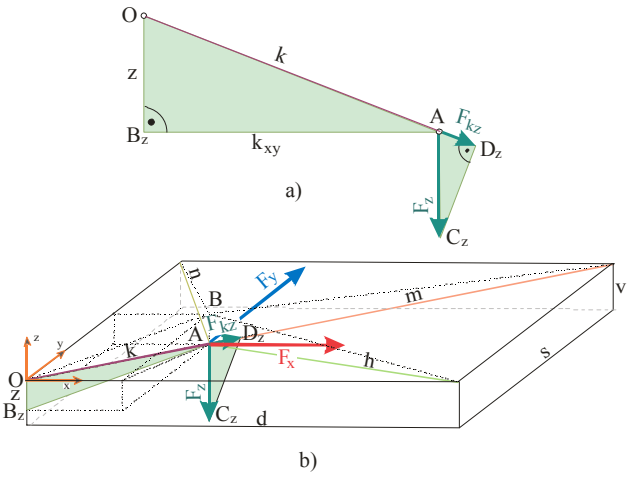

Figure 6. a) A characteristic triangle in the z - k plane, b) A characteristic triangle in the 3D space

The other two sides of the OAB_z triangle have the sizes z and $k_{xy} = \sqrt{x^2 + y^2}$.

The component of the external force F in the z direction is F_z and the projection of the force F_z on the k direction is F_{kz} which can be seen in Fig.6.

The similarities of the two triangles in Fig.6 produce the following relations:

$$\frac{z}{k} = \frac{F_{kz}}{F_z}. \tag{12}$$

$$F_{kz} = \frac{z}{k} \cdot F_z. \tag{13}$$

The force F_k is a sum of the previously defined components and it is expressed in the following equation:

$$F_k = F_{kx} + F_{ky} + F_{kz} = \frac{x}{k} \cdot F_x + \frac{y}{k} \cdot F_y + \frac{z}{k} \cdot F_z \tag{14}$$

By using the geometric properties of similar triangles, and the methodology from the previous procedure, we have defined the forces F_h, F_m, and F_n, in the other three ropes.

$$F_h = F_{hx} + F_{hy} + F_{hz} \tag{15}$$

$$F_m = F_{mx} + F_{my} + F_{mz} \tag{16}$$

$$F_n = F_{nx} + F_{ny} + F_{nz} \tag{17}$$

The forces in the ropes which carry the camera are shown in Fig.3. The important property of the RFCPR system is that the directions k have two parallel ropes (as shown in Fig.1), which means that the total force k direction has two components. This means that the total force F_k in the k direction has two components of the same value $\Diamond \cdot F_k$.

The dynamic balance between the force F_k in the k rope direction and the external force F is thus described. See Figures 4-6.

The main forces F_1, F_2 or F_3 are generated from the forces in the ropes: $\Diamond \cdot F_k$, F_h, F_m and F_n and they produce the load on the shaft of the related motors through the radius R_1, R_2, and R_3 of the corresponding winder.

The native of the mechanism construction creates dependency of the forces F_k, F_h, F_m and F_n, and the main motor load moments M_1, M_2, and M_3.

Following this procedure, the relationship between the main motor load moment and the total external force can be defined in a vector form. See equation (18).

$$\begin{bmatrix} F_1 \cdot R_1 \\ F_2 \cdot R_2 \\ F_3 \cdot R_3 \end{bmatrix} = \begin{bmatrix} O_{\Diamond F11} & O_{\Diamond F12} & O_{\Diamond F13} \\ O_{\Diamond F21} & O_{\Diamond F22} & O_{\Diamond F23} \\ O_{\Diamond F31} & O_{\Diamond F32} & O_{\Diamond F33} \end{bmatrix} \cdot \begin{bmatrix} F_x \\ F_y \\ F_z \end{bmatrix}. \qquad (18)$$

The moment mapping matrix $O_{\Diamond F}$ has a dimension (m) and depends only on the geometry of the observed mechanism and selected motion trajectory of the camera carrier during the manipulator task. The determination of the matrix $O_{\Diamond F}$ is complex and it highly depends on the imagination of researchers, which can cause errors. In order to define equation (18), the Lagrange's principle of virtual work has been used to find the relation between internal and external forces.

The connection between the main load moment M_F and the external force F is established. See equation (19).

$$M_F = O_{\Diamond F} \cdot F \qquad (19)$$

By substituting equations (19) into equation (15), the dynamic model of RFCPR has been generated:

$$u = G_v \cdot \ddot{\varphi} + L_v \cdot \dot{\varphi} + S_v \cdot O_{\Diamond F} \cdot F\,. \qquad (20)$$

The matrix $O_{\Diamond F}$ represents a strong coupling between the presented motors.

Through the comparative results, it will be shown how motor selection can significantly affect the motion dynamics of the camera carrier. This emphasizes the importance of selecting a motor type as a very important component of the CPR system.

Control law is selected by the local feedback loop for the position and velocity of the motor shaft in the following equation:

$$u_i = K_{lpi} \cdot (\theta_i^{\circ} - \theta_i) + K_{lvi} \cdot (\dot{\theta}_i^{\circ} - \dot{\theta}_i) \qquad (21)$$

The ORVER program package

The RFCPR system is modeled and analyzed by the ORVER software package. The ORVER software package is used for the validation of applied theoretical contributions.

The ORVER software package includes three essential modules, which are the kinematic, dynamic and motion control law solvers for the RFCPR system.

The most important element of the RFCPR system is the motor mathematical model which is an integral part of the ORVER software package. Through the simulation results it is shown that the dynamic characteristics of the motor significantly affect the response of the system and its stability.

The RFCPR system presented in Figures 1 and 2 is analyzed. In order to make the results comparable, the simulation is made for the same desired system parameters defined in the Designation. The motors are selected by Heinzman SL100F and the gear boxes are HFUC14-50-2A-GR+belt.

Some important characteristics of the RFCPR system are: gravitational acceleration $g = 9.81(\mathrm{m/s^2})$, sample time $dt = 0.0001(\mathrm{s})$, winch radius $R_i = 0.15(\mathrm{m})$, rotor circuit resistance $R_{ri} = 0.917(\Omega)$, back electromotive force constant $C_{Ei} = 3.3942(V/(\mathrm{rad/s}))$, constant of the moment proportionality $C_{Mi} = 2.5194(\mathrm{Nm/A})$, coefficient of viscous friction $B_{Ci} = 0.0670(\mathrm{Nm/(rad/s)})$, moment of inertia for the rotor and the gear box $J_{ri} = 1.5859(\mathrm{kgm^2})$, motor inertia characteristic $G_{vi} = \dfrac{J_{ri} \cdot R_{ri}}{C_{Mi}} = 0.1787$, motor damping characteristic $L_{vi} = \dfrac{R_{ri} \cdot B_{Ci}}{C_{Mi}} + C_{Ei} = 3.4186$, motor geometric characteristic $S_{vi} = \dfrac{R_{ri}}{C_{Mi}} = 0.364$, mass of the camera carrier $m = 1(\mathrm{kg})$, length of the recorded field $d = 3.2(\mathrm{m})$, width of the recorded field $s = 2.2(\mathrm{m})$, height of the recorded field $v = 2.0(\mathrm{m})$, initial deviation of the motor angular position $\delta\theta_{i\Xi} = 0(\mathrm{rad})$, $\delta\dot{\theta}_{i\Xi} = 0(\mathrm{rad/s})$, positional $K_{lpi} = 4200$, velocity $K_{lvi} = 130$ amplification for motion control and the factor that characterizes two parallel guided ropes $\Diamond = 0.5$.

The system is coupled at the reference level and its mathematical model is defined by equations (1-20).

The RFCPR model has been analyzed using the selected camera trajectory.

The camera moves in the 3D space (x, y and z directions). The camera carrier has the starting point $p^{\circ}_{start} = [2.5 \;\; 0.5 \;\; -1.2](\mathrm{m})$, and the end point $p^{\circ}_{end} = [0.7 \;\; 1.7 \;\; -0.2](\mathrm{m})$ (see Fig.7a)). The camera motion velocity has a trapezoid form and $\dot{p}^{\circ}_{\max} = 0.625(\mathrm{m/s})$, as shown in Fig.7b).

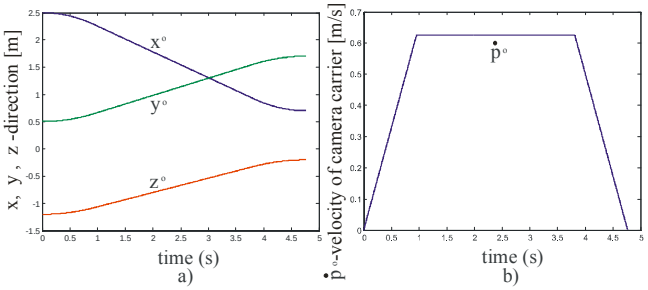

Figure 7. The reference trajectory motion of a) position x°, y°, z°, b) velocity $\dot{p}^{\circ}_{\max} = 0.625(\mathrm{m/s})$ of the camera carrier

The radii of the winches for all three motorized pulleys are mutually equal. Their values are: $R_1 = R_2 = R_3 = 0.15(\mathrm{m})$. All three motor's angular positions θ_1, θ_2, and θ_3 are involved in the coordinated task

generation. This clearly represents a proof that all of these motions are mutually coupled. The system responses, for the first and the second Example are shown in Figures 8 and 10, respectively. The perturbation force that acted on the camera carrier in Example 2 is presented in Fig.9.

These results are comparable and therefore shown in Table 1.

Each example has six pictures related to the:

a) camera carrier position at the reference and the real frames,
b) motor shaft position at the reference and the real frames,
c) forces in the ropes at the reference and the real frames,
d) deviation between the real and the reference trajectory of the camera carrier,
e) deviation between the real and the reference trajectory of the motor shaft positions,
f) control signals at the reference and the real frames.

Table 1. Comparison of two selected Examples

Example	Figure	Perturbation force
1	8	no
2	9, 10	yes

***Example* 1**

The first Example shows a good response. Motor 1 goes into saturation (reaches the value of the minimum voltage $u_{\max 1} = -24(\mathrm{V})$) during a short time period of the motion.

This is reflected on the system response, but generally the tracking error of the motor angular positions and the camera carrier motion with respect to the desired values are in the acceptable range. See Fig.8.

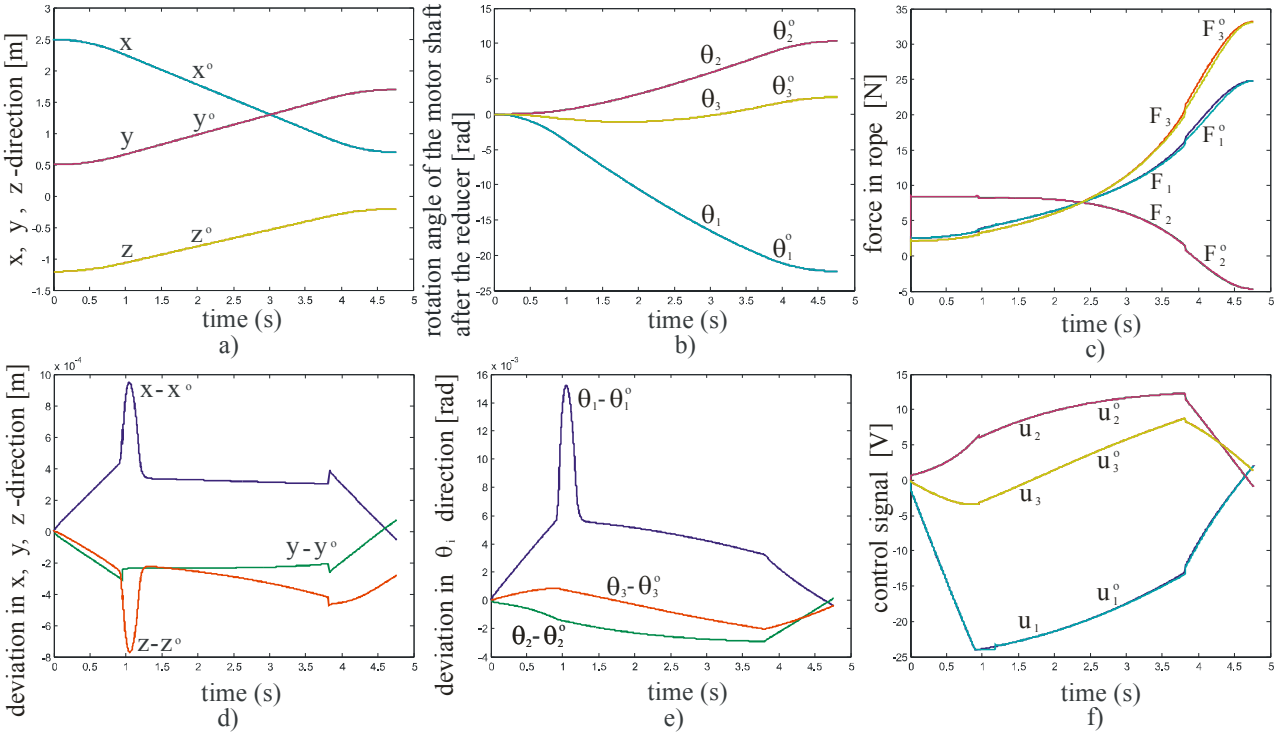

Figure 8. Example 1

***Example* 2**

All system and control parameters are the same as in Example 1. The camera carrier is under the influence of the disturbance force

$$F_p = \left[50 \cdot \sin(4 \cdot \pi \cdot t) + \frac{2}{3} \cdot 50 \cdot \sin(8 \cdot \pi \cdot t) + \frac{2}{3} \cdot 50 \cdot \sin(16 \cdot \pi \cdot t) \;\; 0 \;\; 0 \right]^T,$$

which simulates the impact of the wind attack. See Fig.9.

The perturbation force has the sine shape and operates only in the x direction, while the components in the y and z directions are zero. The motion response of the camera carrier has the oscillatory characteristics and the all three motors angular positions are caused by the sinusoidal disturbance force.

There is a very good tracking of the desired trajectory at the camera carrier reference frame and at the motor motion reference frame, until the moment when Motor 1 enters the saturation. See Fig.10.

Perturbing forces may represent a significant disturbance to the system, depending on their intensity and the change dynamics.

The space observing CPR system being developed in the Mihajlo Pupin Institute is a part of a more complex system.

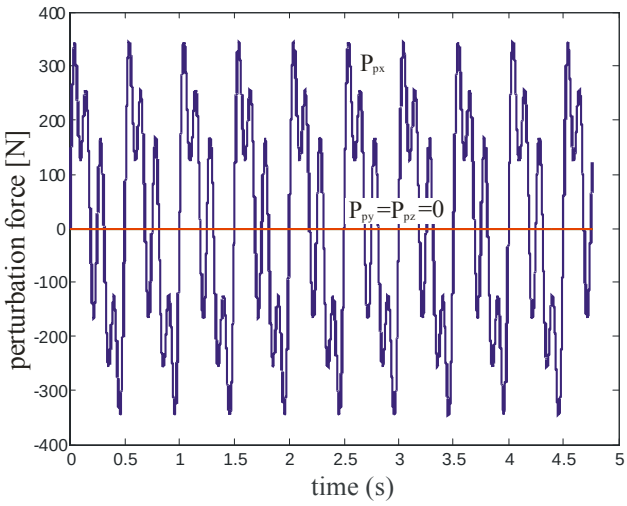

Figure 9. Perturbation force

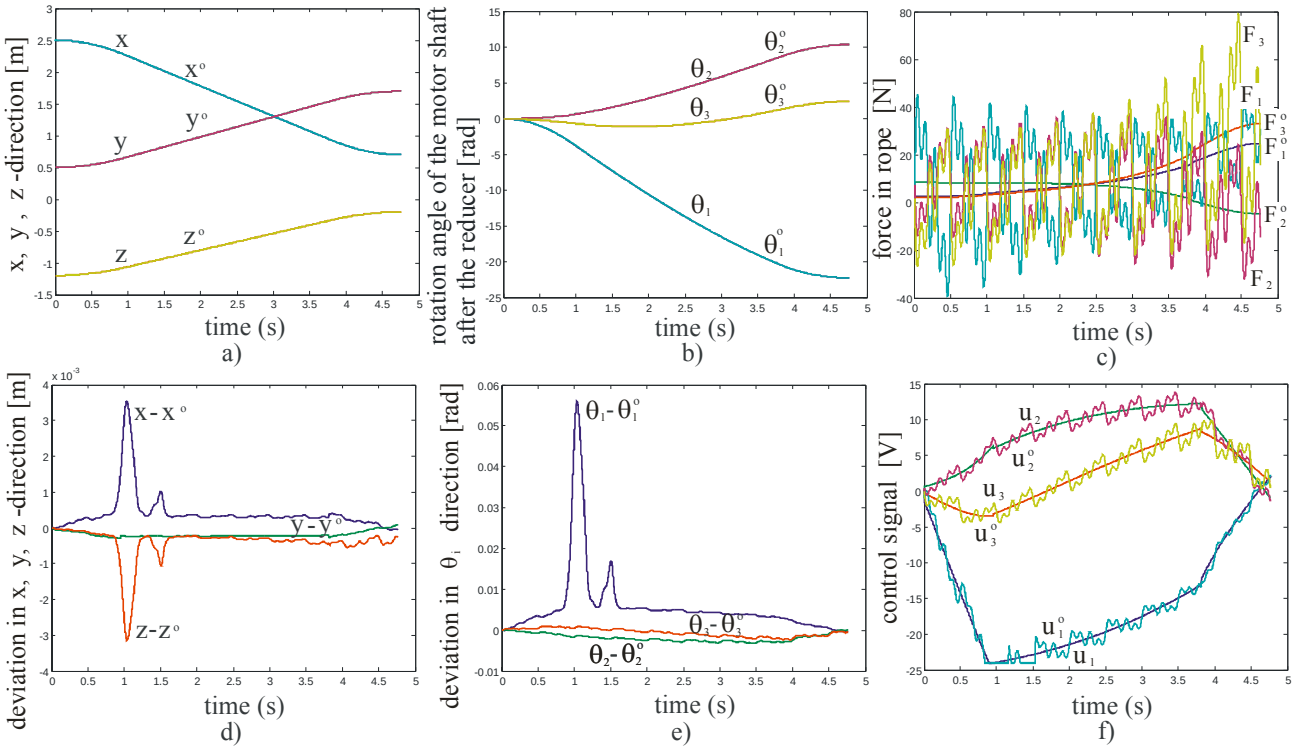

Figure 10. Example 2

Conclusion

The kinematic model is defined for the monitored Cable-suspended Parallel Robot named the RFCPR system. The generalized coordinates selected for the RFCPR model are the motors angular positions θ_1, θ_2, θ_3, named the internal coordinates. The camera motion is defined in the Cartesian space, described with the x, y, z coordinates, named the external coordinate system. The relation between the internal and the external coordinate system is described by the Jacobian matrix J_F. This relation represents the direct and inverse kinematic model of the RFCPR system.

The relation between the forces in the ropes and the forces acting at the camera carrier is described by the Lagrange principle of virtual work. This calculation shows that in this relation the Jacobian matrix is involved as well.

This relation is used for generating the dynamic model of this system. It can be concluded that the geometry of the mechanism significantly influences the form of the kinematic and dynamic model of the considered mechanism. The motor type significantly affects the response of the system or the accuracy of the trajectory tracking.

The ORVER software package has been developed and used for an individual analysis of the CPR model from various aspects such as selecting different workspace dimensions, camera carrier mass, external disturbances, choice of control law, reference trajectory, singularity avoidance and many other characteristics.

Two significant examples have been used for the analysis and validation of the RFCPR system

In Example 1, the first motor goes into saturation (minimum voltage) during certain period of time. During this period of time, the camera motion defers from the desired trajectory.

The significance of Example 2 is that the camera carrier is under the influence of the disturbance force while in Example 1 the camera moves without the influence of disturbance. All other system and control parameters are the same as in Example 1. The disturbance force has the sine shape and operates only in the x direction.

Until the moment when Motor 1 enters the saturation, tracking of the desired trajectory is very good both at the camera carrier and at the motor motion reference frame. During the period when Motor 1 is in saturation, the tracking of its angular position is very bad. This indirectly causes poor tracking of the desired trajectory in the Cartesian space in all three directions, x, y and z.

The oscillatory characteristics of the system response are caused by the dynamics of the disturbing force changes. Entering the saturation of the first motor is caused by the choice of a motor which is not good enough to achieve the desired velocity of the camera carrier.

Acknowledgment

This research has been supported by the Ministry of Education, Science and Technological Development of the Government of the Republic of Serbia through the following two projects: Grant TR-35003 "Ambientally intelligent service robots of anthropomorphic characteristics", by Mihajlo Pupin Institute, University of Belgrade, Serbia and Grant OI-174001 "The dynamics of hybrid systems of complex structure", by Institute SANU Belgrade and Faculty of Mechanical Engineering University of Nis, Serbia, and partially supported by the project SNSF Care-robotics project No. IZ74Z0-137361/1 by Ecole Polytechnique Federale de Lausanne, Switzerland.

References

[1] BORGSTROM,P.H., BORGSTROM,N.P., STEALEY,M.J., JORDAN,B., SUKHATME,G., BATALIN,M.A., KAISER,W.J.: *Discrete Trajectory Control Algorithms for NIMS3D, an Autonomous Underconstrained Three-Dimensional Cabled Robot*, Proceedings of the 2007 IEEE/RSJ International Conference on Intelligent Robots and Systems, San Diego, CA, USA, 2007.

[2] BRUCKMANN,T., MIKELSONS,L., SCHRAMM,D., HILLER,M.: *Continuous workspace analysis for parallel cable-driven Stewart-Gough platforms*, Special Issue: Sixth International Congress on Industrial Applied Mathematics (ICIAM07) and GAMM Annual Meeting, Zurich, 2007, 7(1).

[3] CARRICATO,M.: *Under-constrained cable-driven parallel robots*, part of book Quarta giornata di studio Ettore Funaioli - 16 luglio 2010, Asterisco, 2011, 443-454.

[4] DJURIĆ,A.M., AL SAIDI,R., ELMARAGHY,W.H.: *Dynamics Solution of n-DOF Global Machinery Model*, Robotics and Computer Integrated Manufacturing (CIM)" Journal, 2012, Vol.28, No.5, pp.621-630.

[5] DJURIĆ,A.M., AL SAIDI,R., EL MARAGHY,W.H.: *Global Kinematic Model Generation for n-DOF Reconfigurable Machinery Structure*, 6th IEEE Conference on Automation Science and Engineering, CASE 2010, Toronto, Canada, August 21-24, 2010.

[6] DUAN,B.Y.: *A new design project of the line feed structure for large spherical radio telescope and its nonlinear dynamic analysis*, Mechatronics, 1998, Vol.9, pp.53-64.

[7] FANG,S., FRANITZA,D., TORLO,M., BEKES,F., HILLER,M.: *Motion control of a tendon-based parallel manipulator using optimal tension distribution*, IEEE/ASME Trans. Mechatron., 2004, 9(3), pp.561-568.

[8] FILIPOVIĆ,M.: *Dynamic of Biped Movement on a Mobile Platform in the Presence Elasticity Elements,* Scientific Technical Review, ISSN 1820-0206, 2008, Vol.58, No. 1, pp.15-24.

[9] FILIPOVIĆ,M.: *New View of the Euler-Bernoulli Equation*, Scientific Technical Review, ISSN 1820-0206, 2009, Vol.59, No.1, pp.41-51.

[10] FILIPOVIĆ,M.: *Analogue between New Formulation of Euler-Bernoulli Equation and Algorithm of Forming Mathematical Models of Robot Motion*, Scientific Technical Review, ISSN 1820-0206, 2010, Vol.60, No.1, pp.19-29.

[11] FILIPOVIĆ,M.: *Relation between Euler-Bernoulli Equation and Contemporary Knowledge in Robotics, Robotica*, 2011, Vol.30, pp.1-13.

[12] FILIPOVIĆ,M., POTKONJAK,V., VUKOBRATOVIĆ,M.: *Elasticity in Humanoid Robotics*, Scientific Technical Review, ISSN 1820-0206, 2007, Vol.57, No.1, pp.24-33.

[13] FILIPOVIĆ,M., VUKOBRATOVIĆ,M.: *Contribution to modeling of* elastic *robotic systems*, Engineering & Automation Problems, International Journal, September 23, 2006, Vol.5, No.1, pp.22-35.

[14] FILIPOVIĆ,M., VUKOBRATOVIĆ,M.: *Complement of Source Equation of Elastic Line*, Journal of Intelligent & Robotic Systems, International Journal, June 2008, Vol.52, No.2, pp.233-261.

[15] FILIPOVIĆ,M.: *The Importance of Modelling an Aerial Robotic Camera*, Scientific Technical Review, ISSN 1820-0206, Military Technical Institute, Belgrade, Serbia, 2012, Vol.62, No.1, pp. 28-37.

[16] GOSSELIN,C., GRENIER,M.: *On the determination of the force distribution in overconstrained cable-driven parallel mechanisms*, Meccanica, An International Journal of Theoretical and Applied Mechanics, Springer, 2011, 46 (1), pp.3-15.

[17] GOSSELIN,C., REN,P., FOUCAULT,S.: *Dynamic Trajectory Planning of a Two–DOF Cable-Suspended Parallel Robot*, 2012 International Conference on Robotics and Automation RiverCentre, Saint Paul, Minnesota, USA, May 14-18, 2012.

[18] GOUTTEFARDE,M., MERLET,J.P., DANEY,D.: *Determination of the wrench-closure workspace of 6-DOF parallel cable-driven mechanisms*, Advances in Robot Kinematics, 2006, 5, pp.315-322.

[19] HEDRIH (STEVANOVIĆ) K.: *Energy transfer in the hybrid system dynamics (energy transfer in the axially moving double belt system)*, Special Issue, ARCH APPL MECH, 2009, Vol.79, No.6-7,pp.529-540.

[20] HEDRIH (STEVANOVIĆ) K.: *Transversal forced vibrations of an axially moving sandwich belt system*, ARCH APPL MECH, Springer, 2008, Vol.78, No.9, pp.725-735.

[21] HEDRIH (STEVANOVIĆ) K.: *Vibration Modes of a axially moving double belt system with creep layer*, J VIB CONTROL, 2008, Vol. 14, pp. 1333-1347.

[22] HEDRIH (STEVANOVIĆ) K.: *Dynamics of multipendulum systems with fractional order creep elements*, Special Issue Vibration and Chaos, J THEOR APP MECH-POL, Warsaw, Poland, 2008, Vol.46, No.3, pp.483-509.

[23] HEDRIH (STEVANOVIĆ) K.: *Dynamics of coupled systems, Nonlinear Analysis: Hybrid Systems*, 2008, Vol.2, No.2, pp.310-334.

[24] HEDRIH (STEVANOVIĆ) K.: *Transversal vibrations of the axially moving sandwich belts*, ARCH APPL MECH, 2007, Vol.77, No.7, pp.523-539.

[25] HEDRIH (STEVANOVIĆ) K.: *Energy analysis in the hybrid system forced regimes*, Proceeding of Institute of Mathematics NANU Ukraine, 2010, Vol. 7, No.3, pp. 90-107.

[26] HEDRIH (STEVANOVIĆ) K.: *Energy and Nonlinear Dynamics of Hybrid System*, Chapter in Book Dynamical Systems and Methods, Edited by Albert Luo, Springer, 2012, Vol.1, pp.29-83.

[27] HIGUCHI,T., MING,A., JIANG-YU,J.: *Application of multi-dimensional wire crane in construction*, In 5th Int. Symp. on Robotics in Construction, Tokyo, June, 6-8, 1988, pp.661–668.

[28] HILLER,M., FANG,S.Q.: Design, analysis and realization of tendon-base parallel manipulators, Mech. Mach. Theory, 2005, Vol.40, pp.429-445.

[29] KOZAK,K., ZHOU,Q., WANG,J.S.: *Static Analysis of Cable-Driven Manipulators With Non-Negligible Cable Mass*, IEEE Transaction on Robotics, June 2006, Vol.22, No.2, pp.425-433.

[30] MERLET,J.P.M., MARIONET,A.: *Family of Modular Wire-Driven* Parallel Robots, Advances in Robot Kinematics: Motion in Man and Machine, 2010, 1, pp.53-61.

[31] MIERMEISTER,P., POTT,A., VERL,A.: *Auto-Calibration Method for Overconstrained Cable-Driven Parallel Robots*, ROBOTIK 2012 - 7th German Conference on Robotics, Munich, Germany, 2012.

[32] OH,S.R., AGRAWAL,S.K.: *A Reference Governor-Based Controller for a Cable Robot Under Input Constraints*, IEEE Transaction on Control Systems Technology, July 2005, Vol.13, No.4, pp.639-645.

[33] POTT,A.: *Forward Kinematics and Workspace Determination of a Wire Robot for Industrial Applications*, Advances in Robot Kinematics: Analysis and Design, 2008, 7, pp.451-458.

[34] RASKOVIĆ,D.: *Theory of oscillations*, Scientific book, Belgrade, Serbia, 1965.

[35] REGA,G.: *Nonlinear vibrations of suspended cables-Part I: modeling and analysis*, ASME, APPL MECH REV, 2004. Vol. 57, No 6, pp. 443-478

[36] REGA,G.: *Nonlinear vibrations of suspended cables-Part II: deterministic phenomena*, ASME, APPL MECH REV, 2004. Vol. 57, No 6, pp. 479-514.

[37] SHIANG,W-J., CANNON,D., GORMAN,J.: *Optimal Force Distribution Applied to a Robotic Crane with Flexible Cables*, Proceedings of the 2000 IEEE International Conference on Robotics & Automation, San Francisco, Ca, April 2000, pp.1948-1954.

[38] SU,X.Y., DUAN, B.Y.: *The Application of the Stewart Platform in Large Spherical Radio Telescopes*, Journal of Robotic Systems by John Wiley & Sons, 2000, Vol.17, No.7, pp.375-383.

[39] SU,X.Y., DUAN, B.Y.: *The mathematical design and kinematics accuracy analysis of a fine tuning stable platform for the large spherical radio telescope, Mechatronics*, 2000, Vol.10, pp.819-834.

[40] YAO,R., TANG,X., WANG,J., HUANG,P.: *Dimensional Optimization Design of the Four-Cable Driven Parallel Manipulator in FAST*, IEEE/ASME Transaction on Mechatronics, 2010, 15(6) pp.932-941.

[41] ZI,B., DUAN,B.Y., DU,J.L., BAO,H.: *Dynamic modeling and active control of a cable-suspended parallel robot*, Mechatronics, 2008, 18, pp.1-12.

Received: 12.10.2013.

Uticaj tipa konstrukcije kablovski vodjenog paralelnog robota na njegov kinematički i dinamički model

Predstavljeni kablovski vodjen paralelni robot nazvan RFCPR sistem je važno i interesantno rešenje za inženjersku i naučnu javnost s obzirom na mogućnost njegovog budućeg razvoja. Odgovarajuća definicija kinematičkog modela sistema, što uključuje trajektoriju, brzinu i ubrzanje, je preduslov za formulaciju dinamičkog modela. Ove tri komponente predstavljaju bazični funkcionalni kriterijum realnog sistema što je opisano sa odgovarajućim geometrijskim relacijama i diferencijalnim jednačinama. Veze izmedju spoljašnjih i unutrašnjih sila su definisane preko Lagranžovog principa virtuelnog rada. Jakobijeva matrica je direktno uključena u primenu Lagranžovog principa virtuelnog rada i generisanje dinamičkog modela RFCPR sistema. Konstrukcija sistema u osnovi definiše njegov kinematički i dinamički model. Softverski paket ORVER je korišćen za uporednu analizu dinamike odziva posmatrane konfiguracije. Analizirani su i predstavljeni rezultati dva različita primera RFCPR sistema. Mogućnosti primene su svakako mnogo šire nego što se može pretpostaviti u ovom trenutku, posebno za vojne ili policijske svrhe.

Ključne reči: **robotizovani sistem, vođenje pomoću kabla, kablovska veza, analiza modela, kinematska analiza, dinamička analiza, Lagranžova metoda, Jakobijeva matrica, softver.**

Влияние типа структуры параллельного робота управляемого путём кабельной системы на его кинематическую и динамическую модели

Показанный параллельный робот управляемый путём кабельной системы, назван RFCPR-системой, является важным и интересным решением для инженерных и научных явных кругов в связи с возможностью его дальнейшего развития. Соответствующее определение кинематической модели системы, в том числе и траектории, скорости и ускорения, является необходимым условием для разработки и определения динамической модели. Эти три составляющие представляют основной функциональный критерий реальной системы, что здесь описывается с соответствующими геометрическими расстояниями и дифференциальными уравнениями. Связи между внешними и внутренними силами определяются путём принципа Лагранжа виртуальной работы. Матрица Якоби принимает непосредственное участие в реализации принципа Лагранжа виртуальной работы и в формировании динамической модели RFCPR-системы. Конструкция системы в основном определяет свои кинематические и динамические модели. Пакет программного обеспечения ORVER использован для сравнительного анализа динамики реагирования наблюдательской конфигурации. Были проанализированы и представлены результаты двух различных примеров RFCPR-системы. Возможности применения , конечно, гораздо больше и шире, чем можно себе представить в этот момент, особенно для военных или полицейских целей.

Ключевые слова: **роботизированная система, управление путём кабельной системы, кабельная связь, анализ модели, кинематический анализ, динамический анализ, метод Лагранжа, матрица Якоби, программное обеспечение.**

Influence du type de construction du robot parallèle guidé par câble à son modèle cinématique et dynamique

Le robot parallèle guidé par câble, présenté dans ce papier, appelé le système RFCR, est une solution importante et intéressante pour les milieux scientifiques et ingénieurs à l'égard des possibilités de son futur développement. La définition adéquate du modèle cinématique de système qui comprend la trajectoire, la vitesse et l'accélération, est la condition préalable pour la formulation du modèle dynamique. Ces trois composantes représentent le critère fonctionnel de base du système réel qui est décrit par les relations géométriques correspondantes ainsi que par les équations différentielles. Les relations entre les forces externes et les forces internes ont été définies au moyen du principe du travail virtuel de Lagrange. La matrice de Jacobien est inclue directement dans l'emploi du principe du travail virtuel de Lagrange et la création du modèle dynamique du système RFCR. La construction du système définit son modèle cinématique et dynamique. Le progiciel ORVER a été utilisé pour l'analyse comparative de la dynamique de réponse de la configuration considérée. On a analysé et présenté les résultats pour les deux différents exemples du système RCFR. Les possibilités d'emploi sont certainement beaucoup plus grandes qu'on suppose en ce moment, en particulier dans les fins militaires ou policiers.

Mots clés: **système robotisé, guidage par câble, connexion par câble, analyse de modèle, analyse cinématique, analyse dynamique, méthode de Lagrange, méthode de Jacobien, logiciel.**